ISSN 1066-3622, Radiochemistry, 2020, Vol. 62, No. 1, pp. 107–118. © Pleiades Publishing, Inc., 2020.

Design, Synthesis, and In Silico Evaluation of Methyl 2-(2-(5-Bromo/chloro-2-oxobenzoxazol-3(2*H*)-yl)-acetamido)-3-phenylpropanoate for TSPO Targeting

P. Srivastava[a,b,*], P. Kumar[b], and Anjani Kumar Tiwari[a,c,]**

[a]*Institute of Nuclear Medicine and Allied Sciences, Delhi, 110054 India*
[b]*Delhi Technological University, Delhi, 110042 India*
[c]*Babasaheb Bhimrao Ambedkar Central University, Lucknow, 226025 India*
**e-mail: pushree14@gmail.com,*
***e-mail: anjanik2003@gmail.com*

Received February 7, 2019; revised April 9, 2019; accepted April 16, 2019

Abstract—The high expression of the translocator protein (TSPO) makes it an ideal target for imaging and therapy. The present study is aimed at optimizing acetamidobenzoxazolone-based TSPO ligands by structural modification to overcome the limitations of TSPO ligands of the first two generations such as nonspecificity and polymorphism. Three different TSPO proteins, 2MGY, 4RYQ, and 4UC1, in the native and mutated form were chosen. Acetamidobenzoxazolones modified with phenylalanine methyl ester (methyl 2-(2-(5-bromo/chloro-2-oxobenzooxazol-3(2*H*)-yl)acetamido)-3-phenylpropanoate, ABPO-Br, ABPO-Cl) through better or comparable docking scores than the known TSPO ligands such as MBMP, FEBMP, FPBMP, and PK11195 are identified as potential TSPO ligands. ABPO-Cl and ABPO-Br were synthesized using phenylalanine methyl ester as a moiety for incorporation of the desired pharmacophoric feature. All the intermediates and final compounds were purified using column chromatography and analytical HPLC (purity > 97%). The purified compounds were characterized by ^{1}H, ^{13}C NMR and mass spectroscopy. Drug likeliness and comparative bioactivity analysis were performed using QikProp through prediction of various properties. Both analogs follow all the five Lipinski rules and three Jogersen's rules predicting their drug likeliness. The other important aspects related to TSPO ligands such as blood–brain barrier penetration and better contrast have been predicted through lipophilicity (QP log P = 2.76 and 2.74 for ABPO-Br and ABPO-Cl, respectively) and serum binding (QP log K_{hsa} = –0.18 and –0.25 for ABPO-Br and ABPO-Cl, respectively). The selectivity and distribution of these TSPO ligands were confirmed by ^{99m}Tc-ABPO-Br dynamic image in New Zealand rabbit. These results have shown that the ABPO analogs have the potential to act as better ligands as compared to known acetamidobenzoxazolone derivatives and would be of interest as a promising starting point for designing compounds for TSPO targeting.

Keywords: TSPO, acetamidobenzoxazolone, phenylalanine methyl ester, ADME, docking, ABPO-Cl, ABPO-Br

DOI: 10.1134/S1066362220010142

INTRODUCTION

The translocator protein (18 kDa, TSPO), previously named as the peripheral benzodiazepine receptor (PBR), was identified as a diazepine peripheral binding site in 1977 [1]. It was distinguished from the central benzodiazepine receptor on the basis of the functional role, unique structure, and cellular location. The TSPO is a 169 amino acid protein arranged in five transmembrane domains [1]. It is primarily located on the outer membrane of mitochondria and also proposed to be located in non mitochondrial site such as nuclear or microsomal site in some cells [2, 3].

TSPO is an important diagnostic and therapeutic target for inflammation and tumor [4–6]. Since TSPO was identified by diazepam, benzodiazepines, and Ro5-4864, several classes of TSPO ligands with diverse structures including isoquinoline carboxamides, benzoazepine, benzothiazepines, indole acetamide, phenoxyphenylacetamide, imidazopyridine acetamides, and pyrazolopyrimidine acetamides have been developed [1, 7, 8].

The isoquinoline carboxamide based ligand PK11195 is currently considered as the state-of-the-art ligand for TSPO. Its most widely studied PET ligand, ^{11}C(*R*) PK11195, from the first generation has a limitation of high nonspecific binding and low brain penetration, resulting in low signal-to-background ratio. Some of the second-generation TSPO ligands could overcome these limitations with higher signal-to-noise ratio compared to PK11195 for improved imaging. Several second-generation TSPO radioligands used in clinical human studies are [^{11}C]DAA1106, [^{18}F]DPA714, [^{11}C]PBR28, and [^{11}C]AC-5216 [9–12].

Although second-generation TSPO ligands have a few advantages over PK11195, there is a problem of intersubject variability due to single nucleotide polymorphism [13]. A new skeleton, acetamidobenzoxazolone (ABO) [14, 15], derived through opening and reorganizing RoS-4864, has been explored for PET application (MBMP, FEBMP and FPBMP) to overcome the problems of intersubject variability [16–21]. ABO has been modified to ABO-amino acid (ABO-AA) for SPECT application by conjugating it with tryptophan methyl ester to maintain the affinity and biocompatibility [22].

This encouraged us to try conjugation of benzoxazolone with other amino acids. Moreover, in a recent study, preference for amino acid transport system LAT1 over other LATs, A, and ASC in normal as well as tumor cells in the uptake of phenylalanine-based radiotracers has been demonstrated through competitive uptake inhibition using inhibitors specific for systems A, ASC, and L [23]. Therefore, phenylalanine can be a better candidate for improving the cell uptake.

Before synthesis, it is important to evaluate the molecule for drug likeliness and TSPO affinity in silico. The literature of drug discovery gives emphasis to combinatorial chemistry and the screening of compounds for drugability involving ADME/toxicity, as the screening of millions of compounds results in a limited number of drug-like compounds. Therefore, it has been advocated that the drugability should be checked before screening for the receptor activity. In current scenario, there is a considerable increase in the application of computer aided drug design methods to predict potential drugs for the diagnosis/treatment of several diseases. In silico prediction of pharmacokinetic parameters, studies of the absorption, distribution, metabolism, and excretion (ADME) have become increasingly important for early screening of potential drug candidates [24].

Around the beginning of 21st century, a simple thumb rule was reported by Lipinski et al. for in silico prediction of oral absorption of a compound through solubility and permeability. As per rule of five, ≈90% of oral molecules clear three out of following four rules: MW ≤ 500 Da, calculated log *P* (clog *P*) ≤ 5 and ≥ 0, hydrogen bond acceptors (HBAs) ≤ 10, and hydrogen bond donors (HBD) ≤ 5 [25, 26]. The bioavailability of molecules is predicted using Jorgensen's rule of 3 (log S_{wat} > –5.7, Apparent Caco-2 permeability >22 nm/s, and number of primary metabolites <7) [27, 28]. Subsequently, a few more in silico properties such as polar surface area (PSA ≤ 140 Å^2) and number of rotatable bonds (≤ 10–20) have been added to expand the correlations with ADME parameters [29].

In silico approaches including docking, quantitative structure–activity relationships, virtual ligand screening, pharmacophore modeling, etc., are other important tools in the discovery and optimization of novel molecules with enhanced affinity and specificity for the selected therapeutic targets [30–33]. Availability of different TSPO PDBs from wild type as well as mutants such as 2MGY, 4RYQ, and 4UC1 have enabled TSPO affinity screening through the docking studies at design level [34–37].

In this study, in continuation of our efforts to develop effective TSPO ligand, we designed a new skeleton, methyl 2-(2-(5-bromo/chloro-2-oxobenzooxazol-3(2*H*)-yl)acetamido)-3-phenylpropanoate by combining 5-bromo/chlorobenzoxazolone with phenylalanine methyl ester and evaluated its ADME properties as well as its affinity for TSPO in silico. Conjugating TSPO pharmacophore (acetamidobenzoxazolone) with methyl phenylalanine could be a promising strategy for drug design, as it may improve the efficacy. Thereafter, conjugation has been carried out in three steps. The product was characterized using NMR, mass spectrometry, and HPLC for further application as TSPO ligand in animal model.

MATERIALS AND METHODS

Chemicals. The chemicals and solvents used in the reactions were purchased from Sigma–Aldrich and Merck. MN60 (60–120 mesh) silica was used for column chromatography, and aluminum plates coated with silica

gel 60 F254 were used for thin layer chromatography (TLC) for monitoring the reaction.

Instrumentation. ^{1}H and ^{13}C NMR spectra were recorded on a Bruker Avance III 600 MHz spectrometer at 600 and 150 MHz, respectively. The mass spectra were taken with an Agilent 6310 system using electrospray ionization. High performance liquid chromatography (HPLC) was carried out on an Agilent 1200 series device using an analytical T3 Waters column (4.6 × 250 mm).

Gamma camera design. For scintigraphic images of ^{99m}Tc-labeled complexes in animal, we used a gamma camera (Symbia, T2, True point SPECT/CT Siemens, INMAS, DRDO, Delhi) equipped with a dual-head low-energy high-resolution parallel-hole collimator interfaced with a computer network system. For image acquisition, an animal was fixed on a mechanical support for standardization of the orientation and position.

Image acquisition parameters. Dorsal ear vein was used for injection in a rabbit. Images were acquired at a defined time point in case of static imaging. For dynamic imaging, acquisition was done for 30 min immediately after injection. Anterior images were acquired with 2 s/frame for 2 min, 15 s/frame for 2 min, and 60 s/frame for 26 min. A 15% window centered on 140 keV (^{99m}Tc peak) with a zoom factor of 1 was used. The matrices used for dynamic imaging were 128 × 128.

Image analysis. The computational data of scintigraphy were extracted and analyzed on a Pegasys workstation (ADAC laboratory). After the image acquisition, the region of interest (ROI) over the organ of interest and the total field of view were drawn.

Ligand preparation. The skeleton was taken from our previous work; it proved its potential for TSPO targeting. Further new analogues were designed and drawn using Chemdraw Ultra 10.0 and were checked for drug likeliness using Lipinski's rule. These analogs and few known TSPO ligands in .mol format were used as input structures for processing in LigPrep, Schrödinger, Maestro LLC 9.1 software. A series of steps in the LigPrep process are as follows: conversions, corrections to the structures, generation of variations in the structures, elimination of unwanted structures, and finally optimization of the structures.

Protein preparation for docking analysis. Prior to docking, identification of the binding site in the target protein is important. This information is taken through the structures of the complexes of the TSPO proteins with its substrate PK11195. The PDB structure files of the proteins are imported and prepared through protein preparation wizard of the Schrödinger software by applying the OPLS_2005 force field. The steps involved in the process of protein preparation are processing, optimization, and minimization of proteins.

The docking protocol was validated through docking back after removing PK11195 from the active site. For the current study, the protein structures were taken from RCSB protein data bank (PDB). Namely, we used 2MGY (wild type TSPO), 4RYQ (wild type TSPO, resolution 1.7 Å), and 4UC1 (mutant TSPO, resolution 1.8 Å).

Docking. Docking is a computational simulation process to predict the preferred orientation of protein–ligand interaction by forming a complex with high stability. Glide, Schrödinger, and Maestro LLC 9.1 offer the speedy and accurate high-throughput virtual screening of several compounds with extremely accurate binding mode predictions.

Both the newly designed analogs as well as few well-known TSPO ligands were subjected to docking with the protein using Glide. The molecules were docked to the active site of TSPO. The molecules docked with negative G Score are suitable for further evaluation. Only the TSPO ligands will have the accurate hydrophobic contact between the ligand and protein, resulting in favorable docking scores.

ADME prediction. The ADME properties were calculated with the aid of QikProp of Schrödinger. It predicts both physicochemical descriptors and pharmacokinetic properties. QikProp provides ranges for all the descriptors and properties of 95% of the known drugs for comparison purpose. It also evaluates the suitability of analogs on the basis of Lipinski's rule of five, which predicts drug-like pharmacokinetic profile for rational drug design. In the present study, the QikProp derived physicochemical properties used for ADME analysis are molecular mass, number of hydrogen bond donors, number of hydrogen bond acceptors, partition coefficients, number of rotatable bonds, molecular volume, etc., which, in turn, predict the properties, for assessing drug likeliness, bioavailability, plasma protein binding, and metabolism. As the molecules are for brain application, we have considered the following predictive properties:

(a) QP log *P* (octanol/water);

(b) QP log *S* (aqueous solubility);

(c) QP log *S* (conformation-independent aqueous solubility);

(d) QP log K_{hsa} (serum protein binding);

(e) QP log BB for blood–brain barrier;

(f) number of primary metabolites;

(g) apparent Caco-2 permeability (nm/s);

(h) apparent MDCK permeability (nm/s);

(i) human oral absorption percentage in GI;

(j) qualitative model for human oral absorption.

Synthesis and Characterization

Synthesis of 5-chlorobenzoxazol-2(3*H*)-one (1). To a solution of 5-chloro-2-aminophenol (500.0 mg, 2.96 mmol) in 150 mL THF, 1,10-carbonyldiimidazole (576.0 mg, 3.55 mmol) was added. The mixture was refluxed with stirring for 2 h. The reaction mixture was quenched by adding 2 m HCl solution after cooling to room temperature. After that, the mixture was extracted with EtOAc. The organic phase was washed with brine, dried over anhydrous sodium sulfate, and filtered. Thereafter, the solvent was removed in vacuo to get the product as a white solid. MS (ESI), *m/z*: 167.8 $[M–H]^+$; calculated *m/z*: 168.0 $[M–H]^+$.

^{1}H NMR (DMSO, 600 MHz): 7.11–7.31 m (3H). ^{13}C NMR (DMSO, 150 MHz):110.3, 111.3, 122.0, 128.2, 132.2, 142.6, 154.7.

Synthesis of methyl 2-(2-chloroacetamido)-3-phenylpropanoate (2). To a solution of L-phenylalanine methyl ester (500.0 mg, 2.32 mmol) in deionized water (10 mL), triethylamine (360 μL, 2.52 mmol) was added with stirring under nitrogen atmosphere on an ice bath over a period of 5 min. To this mixture, chloroacetyl chloride (205 μL, 2.52 mmol) in dichloromethane (10 mL) was added dropwise over a period of 1 h, and the reaction was carried out for 4 h. Thereafter, the mixture was extracted with dichloromethane. The organic layer was washed twice with deionized water and brine solution. After washing, the organic layer was dried over anhydrous sodium sulfate. After filtration, the solvent was removed in vacuo, checked by TLC using $CHCl_3$/MeOH (9 : 1, v/v) as the mobile phase, and purified by silica gel column chromatography using 100% $CHCl_3$ as eluent. MS (ESI), *m/z*: 254.0 $[M–H]^+$; calculated *m/z*: 254.1 $[M–H]^+$. ^{1}H NMR ($CDCl_3$, 600 MHz): 3.11–3.20 m (2H), 3.74 s (3H), 3.98–4.04 m (2H), 4.86–4.90 m (1H), 7.02–7.33 m (6H). ^{13}C NMR ($CDCl_3$, 150 MHz): 37.8, 42.4, 52.5, 53.4, 127.3, 128.7, 129.2, 135.4, 165.6, 171.3.

Synthesis of methyl 2-(2-(5-chloro-2-oxobenzooxazol-3(2*H*)-yl)acetamido)-3-phenylpropanoate, ABPO-Cl (3). To a solution of 5-chlorobenzoxazol-2(3*H*)-one (250.0 mg, 1.48 mmol) and K_2CO_3 (306.0 mg, 2.22 mmol) in DMF (5 mL), methyl 2-(2-chloroacetamido)-3-phenylpropanoate (415.2 mg, 1.63 mmol) was added with cooling on an ice bath. The reaction mixture was stirred at 60–70°C for 3 h. Thereafter, the reaction mixture was cooled to room temperature before adding water. A 1 : 1 mixture of toluene and ethyl acetate was used as an extractant. The organic layer was washed with water and brine and was dried over anhydrous sodium sulfate. The solvent was removed in vacuo after filtration, and the product was purified by silica gel column chromatography using $CHCl_3$/EtOAc (4 : 1, v/v) as eluent. MS (ESI), *m/z*: 387.1 $[M–H]^+$; calculated *m/z*: 387.1 $[M–H]^+$. ^{1}H NMR ($CDCl_3$, 600 MHz): 3.50–3.60 m (2H), 3.86 s (3H), 4.19–4.27 m (2H), 5.07–5.10 m (1H), 6.96–7.33 m (8H). ^{13}C NMR ($CDCl_3$, 150 MHz): 34.0, 51.2, 53.2, 54.4, 121.3–148.8 (10 peaks), 155.3, 168.1, 168.6.

Synthesis of 5-bromobenzoxazol-2(3*H*)-one (4). To a solution of 4-bromo-2-aminophenol (500.0 mg, 2.66 mmol) in 150 mL of THF, 1,10-carbonyldiimidazole (518.0 mg, 3.19 mmol) was added. The mixture was refluxed with stirring for 2 h. The reaction mixture was quenched by adding 2 m HCl solution after cooling to room temperature. EtOAc was used for the extraction. The organic phase was washed with brine, dried over anhydrous sodium sulfate, and filtered. Thereafter, the solvent was removed in vacuo to get the product as white solid. MS (ESI), *m/z*: 211.7 $[M–H]^+$; calculated *m/z*: 211.9 $[M–H]^+$. ^{1}H NMR (DMSO, 600 MHz): 7.20–7.28 m (3H). ^{13}C NMR (DMSO, 150 MHz): 111.7, 112.9, 115.8, 124.8, 132.5, 143.0, 154.6.

Synthesis of methyl 2-(2-(5-bromo-2-oxobenzooxazol-3(2*H*)-yl)acetamido)-3-phenylpropanoate, ABPO-Br (5). To a solution of 5-bromobenzoxazol-2(3*H*)-one (250.0 mg, 1.17 mmol) and K_2CO_3 (242.2 mg, 1.76 mmol) in DMF (5 mL), methyl 2-(2-chloroacetamido)-3-phenylpropanoate (328.2 mg, 1.29 mmol) was added with cooling on an ice bath. The reaction mixture was stirred at 60–70°C for 3 h. Thereafter, the reaction mixture was cooled to room temperature before adding water. A mixture of toluene and ethyl acetate in 1 : 1 ratio was used as extractant.

The organic layer was washed with water and brine and dried over anhydrous sodium sulfate. The solvent was removed in vacuo after filtration and was purified by silica gel column chromatography using $CHCl_3$/EtOAc (4 : 1, v/v) as an eluent. MS (ESI), *m/z*: 431.3 $[M–H]^+$; calculated *m/z*: 431.0 $[M–H]^+$. ^1H NMR ($CDCl_3$, 600 MHz): 3.49–3.60 m (2H), 3.86 s (3H), 4.19–4.27 m (2H), 5.06–5.10 m (1H), 6.91–7.33 m (8H). ^{13}C NMR ($CDCl_3$, 150 MHz): 34.0, 51.2, 53.2, 54.4, 112.6–149.3 (10 peaks), 155.3, 168.0, 168.5.

Radiolabeling protocol. Radioloabeling was performed using method mentioned in the literature [38, 39]. 1 mL of a 1×10^{-2} m $SnCl_2 \cdot 2H_2O$ solution was added to 200 μL of a 3 mM cold ligand solution. Then, 2 mCi of sodium pertechnetate in 100 μL of saline was added. 0.1 m $NaHCO_3$ was used for pH adjustment to 7, and the content was manually shaken and kept at room temperature for 20 min. An ITLC-SG strip as a stationary phase and acetone and PAW (pyridine–acetic acid–water in 3 : 5 : 1.5 ratio) as a mobile phase were used to determine the complexation with ^{99m}Tc and the purity of the labeled compound. Count measurement was done by cutting the ITLC strip into 0.1-cm segments.

Animal studies. Animals were supplied by the Experimental Animal Facility (EAF) of the Institute of Nuclear Medicine and Allied Sciences (INMAS), Delhi. The animals were maintained as per the regulations of the Committee for the Purpose of Control and Supervision of Experiments on Animals (CPCSEA). All the animals were maintained on standard diet (Hindustan Lever Ltd, Mumbai, India) and water. They were kept in the animal house of the institute, which was maintained at 22 ± 2°C and 50% humidity under 12 h dark/light cycles.

Scintigraphy studies. The scintigraphy studies of ^{99m}Tc-labeled complexes were carried out with a New Zealand rabbit. 0.2 mCi of labeled complex was injected intravenously through the ear vein, and images were acquired for 30 min post injection of the radiocomplex.

RESULTS AND DISCUSSION

A new series of acetamidobenzoxazolone–phenylalanine ligands (ABPO, methyl 2-(2-(5-bromo/chloro-2-oxobenzoxazol-3(2*H*)-yl)acetamido)-3-phenylpropanoate) have been designed, evaluated for drug likeliness on the basis of predictive ADME properties in silico, synthesized, and assessed for their affinity toward TSPO through docking. ABPO consists of benzoxazolone and phenylalanine methyl ester moieties coupled by the acetamide group. Two analogs substituted with chlorine or bromine at the 5-position of benzoxazolone have been prepared. The choice of the chloro analog was governed by the fact the presence of chlorine in several TSPO ligands, whereas the bromo analog can provide opportunity to further optimize the property through the substitution reaction. The predicted affinity for TSPO and the drug likeliness properties of the ABPO skeleton were found to be appropriate for the biomedical application in of TSPO overexpression.

It is important to know the pharmacokinetic profile of any molecule to be used in vivo conditions, which can be studied through ADME properties in silico. Often drugs fail to enter the market because of poor pharmacokinetic profile. Thus, it is imperative to design the compound with easy transportability to desired site, proper interaction at the desired site, no or minimal metabolism before the action, and final excretion after the expected action. The prediction of the desired ADME properties at early stages of drug discovery using computer-aided drug design methods reduces the chances of failure of compound at later stages. This has further advantage of low cost and less time required for wet screening.

As we are targeting the receptors/proteins that are found on the outer mitochondrial surface of glial cells, our molecules should be able to reach glial cells of brain. This means that their ability to cross the blood–brain barrier (BBB) is essential and that their lipophilicity should be optimum, as lipophilic substances are required to cross the BBB. During this process, the transportation/binding pattern with human serum is also important for consideration.

The ligands ABPO-Cl/Br satisfy the pharmacological properties of 95% of available drugs available in Schrödinger database. The drug likeliness or capability for becoming a good drug candidate for clinical application was predicted by Lipinski's rule of 5, which is normally used in CADD analysis. ABPO-Cl and ABPO-Br follow all the five rules of Lipinski, reflecting its drug-like properties. Additionally, hydrogen bond acceptors are well within the acceptable proposed limit of 10 for Lipinski's rule. However, QP log *P*, an important property for molecule to cross the blood–brain barrier, is followed by both the designed ligands: 2.74 and 2.76 for bromo and chloro analogs, respectively (see table).

Table 1. Predictive values of discussed properties of known and designed TSPO ligands

Predictions for properties:	Range for 95% of drugs	DAA1106	DPA–713	FGIN–127	PBR06	PBR28	PBR111	PK11195	RoS–4864	ABPO–Br	ABPO–Cl
Solute molecular volume, Å^3	500.0 to 2000.0)	1161.72	1200.85	1501.22	1200.35	1124.07	1307.20	1129.76	941.48	1172.97	1144.621
QP log *P* for octanol/water	–2.0 to 6.5	4.805	3.546	7.019	5.148	4.017	5.118	5.019	3.315	2.76	2.741
QP log K_{hsa}, serum protein binding	–1.5 to 1.5	0.356	0.032	1.318	0.468	0.088	0.39	0.658	0.281	–0.181	–0.256
QP log BB for brain/blood	–3.0 to 1.2	0.056	–0.193	–0.561	0.041	–0.211	0.068	0.102	0.362	–1.092	–0.808
Number of primary, etabolites	1.0 to 8.0	4	4	1	5	5	2	0	1	3	3
QP log s for aqueous solubility	–6.5 to 0.5	–4.046	–3.966	–7.376	–4.834	–4.093	–6.220	–5.319	–4.411	–4.060	3.723
QP log s conformation independent	–6.5 to 0.5	–6.230	–4.447	–7.174	–6.230	–4.884	–5.771	–5.670	–4.651	–5.541	–4.619
Apparent Caco–2 permeability, nm/s	<25 poor, >500 great	5888	2290	2441	6015	3854	3783	4561	2683	248	477
Apparent MDCK permeability (nm/s)	<25 poor, >500 great	6080	1889	3154M	6062	2126	10000	4375	8755	422M	719
Lipinski's rule of 5 violations	Maximum is 4	0	0	1	1	0	1	1	0	0	0
Jorgensen's rule of 3 violations	Maximum is 3	0	0	1	0	0	1	0	0	0	0
Percentage of human oral absorption in GI (±20%)	<25% is poor	100	100	100	100	100	100	100	100	86	91
Qualitative model for human oral absorption	>80% is high	>8 0	>8 0	>8 0	>8 0	>8 0	>8 0	>8 0	>8 0	>8 0	>8 0

Bioavailability prediction. The computed parameters useful for predicting oral absorption are aqueous solubility, conformation-independent aqueous solubility, percentage of human oral absorption in GI, qualitative model for human oral absorption, and compliance with Jorgensen's rule of three.

Out of all known ligands taken for comparison purpose, only two are violating this rule, namely, QP log $S > -5.7$ (–7.4 for FGIN-127 and –6.22 for PBR111). For the designed ligands, the solubilities QP log S range from –4.06 to –3.72; i.e., the solubility of the ligands is better than, or comparable to that of the known ligands.

The Caco-2 permeability for the designed ligands is 248 and 477 nm/s, and for the known ligands it is between 2290 and 6015 nm/s, i.e., much greater than 25 nm/s, the limit of poor permeability as mentioned by the software. The other parameter responsible for absorption, the conformation-independent QP log S values for the designed molecules (–4.62 and –5.54 for the chloro and bromo analogs, respectively) are comparable to those of the known ligands (–7.17 to –4.44). The the percentage human oral absorption in GI is also reasonably good: >85 for the proposed ligands and 100 for the known ligands. Even qualitative model for the human oral absorption predicts high oral absorption.

The molecular flexibility is related to the number of rotatable bonds, which is associated with the bioavailability (increases with a decrease in the number of rotors). Their number in the designed molecule is 6, which is comparable to the known TSPO ligands such as DAA1106, PBR06, and PBR28. However, some known ligands have either high (12 for FGIN-127) or low (0 for RoS-4864) number of rotatable bonds. There is certain optimum number of rotatable bonds to bind in the pocket of the receptor, as there is loss in entropy on binding because of conformational restriction in case of flexible molecules. As the molecule is intended for diagnostic application, too low number of rotatable bonds may lead to stickiness to the target receptor. Therefore, the designed ligands with six rotatable bonds also seem to be suitable for diagnostic purpose (Table 1).

Prediction of the blood–brain barrier (BBB) penetration. As the molecules proposed have potential application for brain, it is mandatory for them to cross the blood–brain barrier. Too polar molecules may be unable to cross BBB. To assess the access of drug to the brain, the blood–brain partition coefficient (QP log BB) is computed. The values for the known TSPO ligands that are from the first and second generations and the designed ligands range from –1.09 to 0.362. This range is permissible for crossing the blood–brain barrier (Table 1).

Prediction of binding with plasma protein. The degree of binding to the blood plasma proteins (like human serum albumin, glycoprotein, lipoproteins, and alpha, beta, and gamma globulins) affects the efficiency of a drug, as it greatly reduces the drug quantity that passes through traverse cell membranes or decreases the diffusion efficiency. Therefore, we predicted the ability of the designed ligands to act on human serum albumin through QP log K_{hsa}. For the known ligands considered, this parameter ranges from 0.032 to 1.31. For PK11195, its value is quite high, i.e., 0.65, resulting in its nonspecific binding, which leads to a poor signal-to-noise ratio in the case of radiolabeled PET ligands. Among the ligands chosen for comparison purpose, DPA-713 and DAA1106 are better with QP log K_{hsa} values of 0.03 and 0.35, leading to better signal-to-noise ratio. The designed skeletons ABPO-Br/Cl (–0.18 and –0.26) exhibit moderate binding, well within the limits (–1.5 to 1.5, Table 1).

Molecular volume. Another crucial factor for binding in the active site of the receptor is the molecular volume. The volume of ligand and that of the active site should match for perfect interaction. To assess the structural compatibility of the molecules with an active site, we analyzed the molecular volume. For RoS4864 and FGIN-127, it is 941 and 1502 Å^3, respectively. However, the molecular volumes for the other known ligands are in the range 1129–1307 Å^3. Both the designed molecules have the molecular volume in the range 1144–1172 Å^3, in which the majority the known ligands are lying. Thus, the proposed ligands have sufficient molecular volume for the ligand–protein interaction (Table 1).

The ligands were synthesized in three steps as shown in Scheme 1. The precursors, 5-bromo/chloro benzoxazol-2(3*H*)-one and methyl 2-(2-chloroacetamido)-3-phenylpropanoate, were synthesized starting from commercially available 4-bromo/chloro-2-aminophenol and phenylalanine methyl ester using cyclization and chloroacetylation reactions and following the procedures reported in the literature with some modiifcation [14, 39]. We used CDI for the cyclization reaction and chloroacetyl chloride with triethyl amine as a base for the chloroacetylation reaction. The final compounds ABPO-Br/Cl were synthesized through alkylation reaction of 5-bromo/chloro-benzoxazolone with methyl

Scheme 1. Synthesis of ABPO-Cl. Reagents: (a) CDI, THF, reflux; (b) chloroacetyl chloride, Et_3N, H_2O/DCM, 0°C–room temperature; (c) K_2CO_3, DMF, 60–70°C, 3 h. APBO-Br was prepared under the same conditions starting from 4-bromo-2-aminophenol instead of 4-chloro-2-aminophenol.

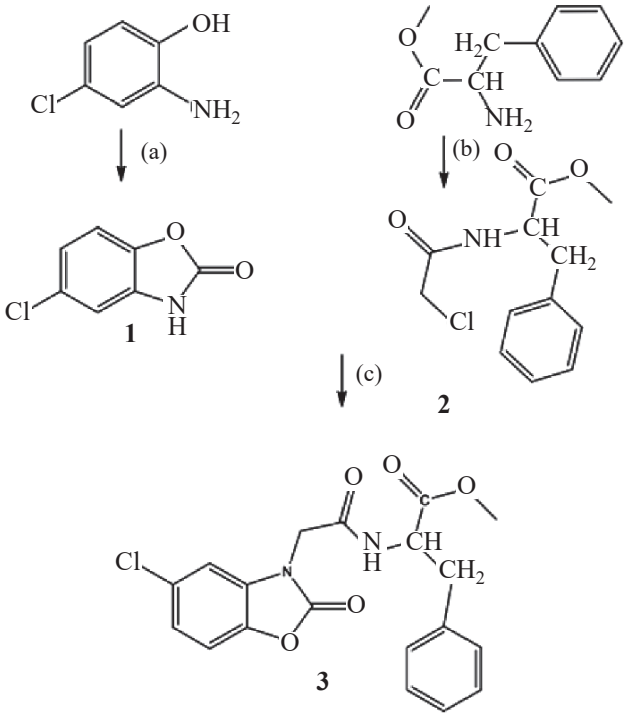

2-(2-chloroacetamido)-3-phenylpropanoate in the presence of K_2CO_3 in DMF. The compounds were purified using column chromatography and preparative HPLC. The chemical purity of the compound was determined using analytical HPLC; the purity was found to be >97%. All the eight aromatic protons of benzoxazolone and benzene moieties were observed in the region of 6–8 ppm. The ^{13}C NMR spectra were consistent with the formula. The C=O carbon signals of benzoxazolone, amide, and ester were observed in the region of 155–169 ppm for both analogs, reflecting the synthesis of ABPO-Cl/Br. The mass spectrometry also confirmed the

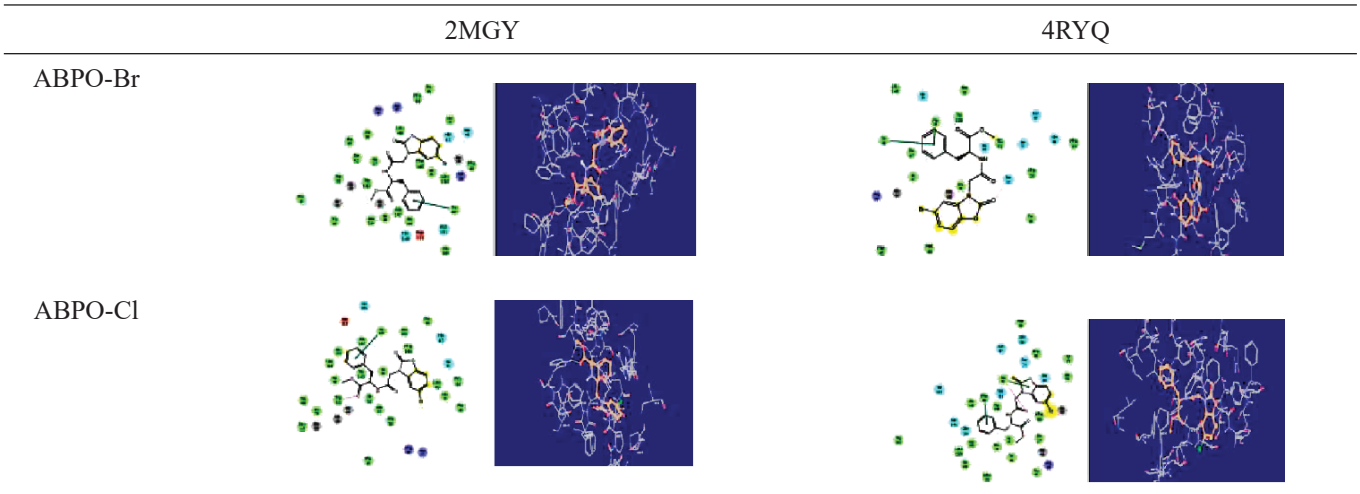

Fig. 1. (Color online) 2D and 3D interaction diagram of ABPO-Br and ABPO-Cl with wild type PDBs 2MGY and 4RYQ.

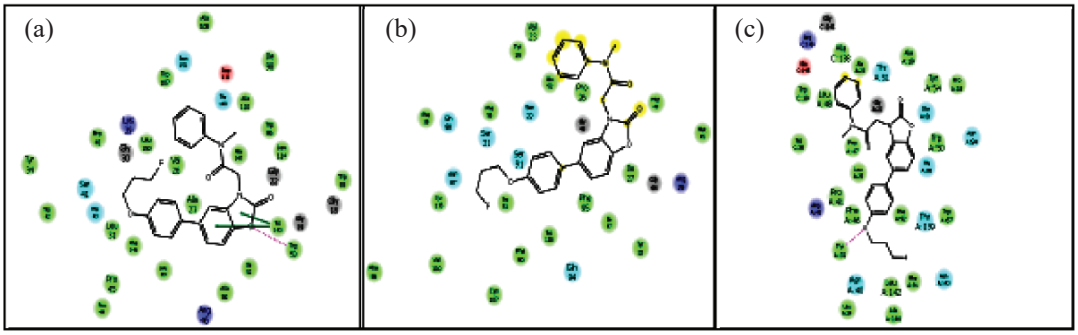

Fig. 2. (Color online) 2D interaction diagram of FEBMP, FPBMP with PDBs: (a) 2MGY, (b) 4RYQ, and (c) 4UC1.

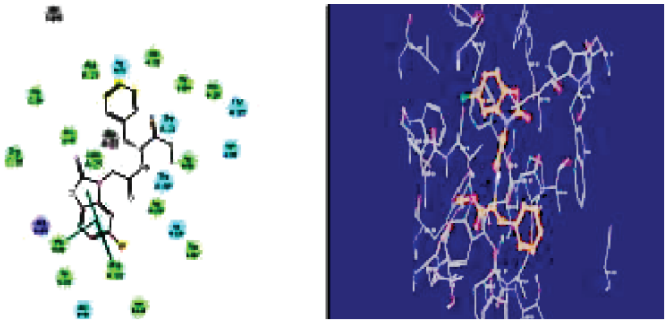

Fig. 3. (Color online) 2D and 3D interaction diagram of ABPO-Cl with mutant type PDB 4UC1.

synthesis: The $[M–H]^+$ peaks of ABPO-Cl and ABPO-Br were observed at *m/z* 387.1 and 431.3, respectively.

The choice of the phenylalanine-based biocompatible ligands was based on their preference for LAT1 over other LATs, A, and ASC system in the uptake mechanism. Validation for TSPO binding/affinity was carried out through docking studies to know about interaction with different amino acid residues of TSPO as compared to other known TSPO ligands. ABPO-Cl/Br demonstrated comparable or better affinity for TSPO in terms of G_{score}, when compared to known ligands like PK11195 and MBMP. Various interactions were observed in docking, including π–π interaction and hydrogen bonding. The phenylalanine aromatic ring is participating in π–π interactions, while one hydrogen bond was observed with the NH group of the acetamidobenzoxalone moiety (Fig. 1, 2).

In docking studies using mutated PDB 4UC1 (A139T) of RsTSPO, the ligands ABPO-Cl/Br showed similarity in interactions with FPBMP/FEBMP. The G_{score} values were comparable for FPBMP, FEBMP, and MBMP. As FEBMP shows no intersubject variability, it can be predicted that the ABPO-Cl/Br could reflect the same. Further studies are required for its validation (Figs. 2, 3).

The radiolabeling study was carried out using the procedure mentioned in the literature with some modification. Complexation of the synthesized ligands with ^{99m}Tc gave 95.4% stability of ^{99m}Tc-ABPO-Br over 24 h. In vitro serum stability clearly demonstrates the stability of the radiolabeled complexes without much transchelation to serum protein like albumin, which was observed to be intact with 92.4% of ^{99m}Tc-ABPO-Br.

The selectivity and distribution of these TSPO ligands were confirmed by tracer techniques in a New Zealand rabbit (dynamic imaging for 30 min, Fig. 4). In brain, significant uptake was observed; it reduced with time. In a nut shell, the uptake was majorly in all the TSPO-rich organs at the initial time point and eventually decreased with time. In excretory organs, the uptakes were initially lower but increased with time till the last time point of the observation.

After intravenous injection of ^{99m}Tc-ABPO-Br, 10-s frames were taken during dynamic studies. Slight uptake in lungs, spleen, and brain is seen in these images. As

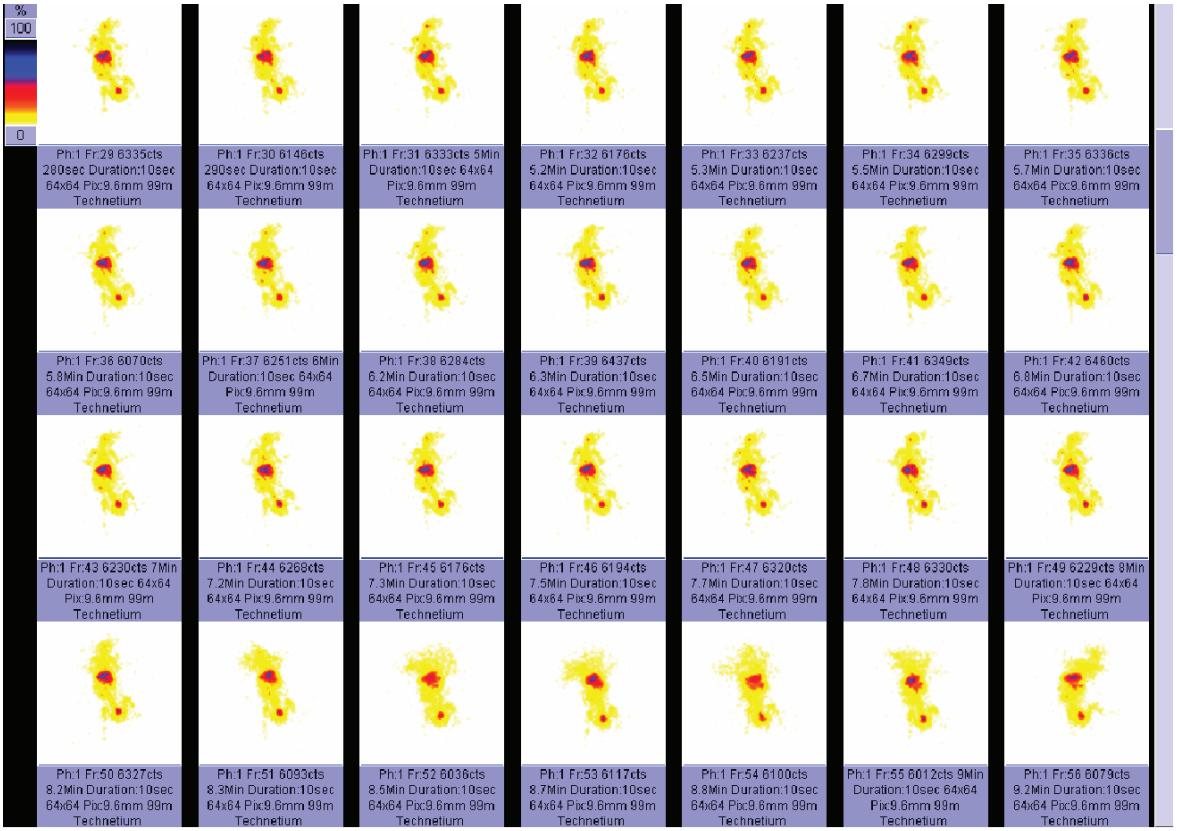

Fig. 4. (Color online) *In vivo* biodistribution of ^{99m}Tc-ABPO-Br in New Zealand rabbit (dynamic image).

the duration of the image capture was 10 s, organs with relatively low uptake were not clearly visualized. Small uptake at later time points was seen, which may be due to fast release kinetics of ^{99m}Tc-ABPO-Br (Fig. 4).

In summary, in silico studies of the modified MBMP skeleton (i.e., ABPO) to evaluate the ADME properties and interaction with TSPO protein, followed by facile synthesis, were carried out for overexpressed TSPO targeting.

CONCLUSION

The goal of the study was synthesis, characterization, and in silico evaluation of acetamidobenzoxazolone–phenylalanine methyl ester, methyl 2-(2-(5-bromo-2-oxobenzooxazol-3(2*H*)-yl)acetamido)-3-phenylpropanoate, for TSPO targeting. The binding affinity for TSPO was assessed through ligand–protein docking and ADME properties by using QikProp modules of Schrödinger software. The biodistribution of these ligands and their selectivity to TSPO were demonstrated in vivo on a New Zealand rabbit. Further preclinical animal studies are required to prove its efficiency as TSPO marker.

ACKNOWLEDGMENTS

The authors are grateful to Dr. Tarun Sekhri, Director of INMAS, Dehli, Dr. A.K. Mishra, Head of the Division of Cyclotron and Radiopharmaceutical Science of INMAS, and Dr. Gaurav Mittal, Head of CCM for providing the facility to carry out the experiments. The authors are also grateful to Dr. Himanshu Ojha, Scientist, Dr. Sonia Gandhi, Scientist, Mr. Sunil Pal, Technical Officer, and Mr. Harish Rawat, INMAS, for their technical support.

FUNDING

The study was supported by INMAS, Delhi, under Task Project ST/15-16/INM-03.

CONFLICT OF INTEREST

The authors declare that they have no conflict of interest.

REFERENCES

1. Papadopoulos, V., Baraldi, M., Guilarte, T.R., Knudsen, T.B., Lacapère, J.J., Lindemann, P., Norenberg, M.D., Nutt, D., Weizman, A., Zhang, M.R., and Gavish, M., *Trends Pharmacol. Sci.,* 2006, vol. 27, pp. 402–409.
2. Li, F., Liu, J., Liu, N., Kuhn, L.A., Garavito, R.M., and Miller, S.F., *Biochemistry,* 2016, vol. 55, pp. 2821–2831.
3. Li, F., Liu, J., Garavito, R.M., and Miller, S.F., *Pharmacol. Res.,* 2015, vol. 99, pp. 404–409.
4. Albrecht, D.S., Granziera, C., Hooker, J.M., and Loggia, M.L., *ACS Chem. Neurosci.,* 2016, vol. 7, pp. 470–483.
5. Kreisl, W.C., Fujita, M., Fujimura, Y., Kimura, N., Jenko, K.J., Kannan, P., Hong, J., Morse, C.L., Zoghbi, S.S., Gladding, R.L., Jacobson, S., Oh, U., Pike, V.W., and Innis, R.B., *Neuroimage,* 2010, vol. 49, pp. 2924–2932.
6. Denora, N., Iacobazzi, R.M., Natile, G., and Margotta, N., *Coord. Chem. Rev.,* 2017, vol. 341, pp. 1–18.
7. Denora, N., Margiotta, N., Laquintana, V., Lopedota, A., Cutrignelli, A., Losacco, M., Franco, M., and Natile, G., *ACS Med. Chem. Lett.,* 2014, vol. 5, pp. 685–689.
8. Milite, C., Barresi, E., Pozzo, E.D., Costa, B., Viviano, M., Porta, A., Messere, A., Sbardella, G., Settimo, F.D., Novellino, E., Cosconati, S., Castellano, S., Taliani, S., and Martini, C., *J. Med. Chem.,* 2017, vol. 60, no. 18, pp. 7897–7909. https://doi.org/10.1021/acs.jmedchem.7b01031
9. Zhang, M.R., Kida, T., Noguchi, J., Furutsuka, K., Maeda, J., Suhara, T., and Suzuki, K., *Nucl. Med. Biol.,* 2003, vol. 30, pp. 513–519.
10. James, M.L., Fulton, R.R., Vercoullie, J., Henderson, D.J., Garreau, L., Chalon, S., Dollé, F., Selleri, S., Guilloteau, D., and Kassiou, M., *J. Nucl. Med.,* 2008, vol. 49, pp. 814–822.
11. Briard, E., Zoghbi, S.S., Imaizumi, M., Gourley, J.P., Shetty, H.U., Hong, J., Cropley, V., Fujita, M., Innis, R.B., and Pike, V.W., *J. Med. Chem.,* 2008, vol. 51, pp. 17–30.
12. Zhang, M.R., Kumata, K., Maeda, J., Yanamoto, K., Hatori, A., Okada, M., Higuchi, M., Obayashi, S., Suhara, T., and Suzuki, K., *J. Nucl. Med.,* 2007, vol. 48, pp. 1853–1861.
13. Owen, D.R., Yeo, A.J., and Gunn, R.N., *J. Cereb. Blood Flow Metab.,* 2012, vol. 32, pp. 1–5.
14. Fukaya, T., Kodo, T., Ishiyama, T., Kakuyama, H., Nishikawa, H., Baba, S., and Masumoto, S., *Bioorg. Med. Chem.,* 2012, vol. 22, pp. 5568–5582.
15. Fukaya, T., Ishiyama, T., Baba, S., and Matsumoto, S., *J. Med. Chem.,* 2013, vol. 56, pp. 8191–8195.
16. Tiwari, A.K., Yui, J., Fujinaga, M., Kumata, K., Shimoda, Y., Yamasaki, T., Xie, L., Hatori, A., Maeda, J., Nengaki, N., and Zhang, M.R., *J. Neurochem.,* 2014, vol. 129, pp. 712–720.
17. Tiwari, A.K., Fujinaga, M., Yui, J., Yamasaki, T., Xie, L., Kumata, K., Mishra, A.K., Shimoda, Y., Hatori, A., Ji, B., Ogawa, M., Kawamura, K., Wang, F., and Zhang, M.R., *Org. Biomol.Chem.,* 2014, vol. 12, pp. 9621–9630.
18. Tiwari, A.K., Ji, B., Fujinaga, M., Yamasaki, T., Xie, L., Luo, R., Shimoda, Y., Kumata, K., Zhang, Y., Hatori, A., Maeda, J., Higuchi, M., Wang, F., and Zhang, M.R., *Theranostics,* 2015, vol. 5, pp. 961–969.
19. Tiwari, A.K., Yui, J., Zhang, Y., Fujinaga, M., Yamasaki, T., Xie, L., Shimoda, Y., Kumata, K., Hatori, A., and Zhang, M.R., *RSC Adv.,* 2015, vol. 5, no. 123, pp. 101447–101454.
20. Kumari, N., Chadha, N., Srivastava, P., Mishra, L.C., Bhagat, S., Mishra, A.K., and Tiwari, A.K., *Chem. Biol. Drug. Des.,* 2017, vol. 90, no. 4, pp. 511–519.
21. Fujinaga, M., Luo, R., Kumata, K., Zhang, Y., Hatori, A., Yamasaki, T., Xie, L., Mori, W., Kurihara, Y., Ogawa, M., Nengaki, N., Wang, F., and Zhang, M.R., *J. Med. Chem.,* 2017, vol. 60, pp. 4047–4061.
22. Srivastava, P., Kaul, A., Ojha, H., Kumar, P., and Tiwari, A.K., *RSC Adv.,* 2016, vol. 6, no. 115, pp. 114491–114499.
23. Hanaoka, H., Ohshima, Y., Suzuki, Y., Yamaguchi, A., Watanabe, S., Uehara, T., Nagamori, S., Kanai, Y., Ishioka, N.S., Tsushima, Y., Endo, K., and Arano, Y., *J. Nucl. Med.,* 2015, vol. 56, pp. 791–797.
24. Kang, F.N., *SpringerPlus,* 2013, vol. 2, article no. 353.
25. Lipinski, C.A., Lombardo, F., Dominy, B.W., and Feeney, P.J., *Adv. Drug. Deliv. Rev.,* 1997, vol. 23, pp. 3–25.
26. Lipinski, C.A., *J. Pharmacol. Toxicol. Meth., 2000*, vol. 44, pp. 235–249.
27. Jorgensen, W.L. and Duffy, E.M., *Adv. Drug Deliv. Rev.,* 2002, vol. 54, pp. 355–366.
28. Jorgensen, W.L. and Duffy, E.M., *Bioorg. Med. Chem. Lett.,* 2000, vol. 10, pp. 1155–1158.
29. Veber, D.F., Johnson, S.R., Cheng, H.Y., Smith, B.R., Ward, K.W., and Kopple, K.D., *J. Med. Chem.,* 2002, vol. 45, pp. 2615–2623.
30. Irwin, J.J. and Shoichet, B.K., *J. Med. Chem.,* 2016, vol. 59, pp. 4103–4120.
31. Pagadala, N.S., Syed, K., and Tuszynski, J., *Biophys. Rev.,* 2017, vol. 9, pp. 91–102.
32. Chaput, L. and Mouawad, L., *J. Cheminform.,* 2017, vol. 9, p. 37.
33. Bhargavi, M., Sivan, S.K., and Potlapally, S.R., *Comp. Biol. Chem.,* 2017, vol. 68, pp. 43–55.

34. Kakkar, D., Tiwari, A.K., Chuttani, K., Kaul, A., Singh, H., and Mishra, A.K., *Cancer Biotherapy and Radiopharmaceuticals*, 2010, vol. 25(6), pp. 645–655.

35. Guo, Y., Kalathur, R.C., Liu, Q., Kloss, B., Bruni, R., Ginter, C., Kloppmann, E., Rost, B.C., and Hendrickson, W.A., *Science,* 2015, vol. 347, pp. 551–555.

36. Li, F., Liu, J., Zheng, Y., Garavito, R.M., and Miller, S.F., *Science,* 2015, vol. 347, pp. 555–558.

37. Tanwar, J., Datta, A., Tiwari, A.K., Thirumal, M., Chuttani, K., and Mishra, A.K., *Bioconjug Chem.,* 2011, vol. 22(2), pp. 244–255.

38. Srivastava, P., Tiwari, A.K., Chadha, N., Chuttani, K., and Mishra, A.K., *Eur. J. Med. Chem.,* 2013, vol. 65, pp. 12–20.

39. Sinha, D., Shukla, G., Tiwari, A.K., Chaturvedi, S., Chuttani, K., Chandra, H., and Mishra, A.K., *Chem. Biol. Drug. Des.,* 2009, vol. 74, pp. 159–164.

40. Singh, S., Tiwari, A.K., Varshney, R., Mathur, R., Hazari, P.P., Singh, B., and Mishra, A.K., *RSC Adv.,* 2015, vol. 5, pp. 41977–41984.